Title
INTERPHASE INTERFACES IN SPINODAL ALLOYS

Authors
Bouchard, M.
Livak, R.J.
Thomas, G.

Publication Date
1971-08-01

Presented at Intern. Conf. on the Structure and Properties of Green Boundaries and Interfaces, IBM Watson Research Center, Yorktown Heights, NY, Aug. 23-25, 1971

LBL-152
Preprint

INTERPHASE INTERFACES IN SPINODAL ALLOYS

M. Bouchard, R. J. Livak and G. Thomas

August 1971

AEC Contract No. W-7405-eng-48

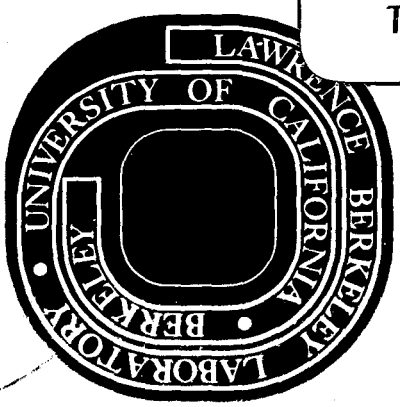

DISCLAIMER

INTERPHASE INTERFACES IN SPINODAL ALLOYS

M. Bouchard, R. J. Livak and G. Thomas

Inorganic Materials Research Division, Lawrence Berkeley Laboratory and Department of Materials Science and Engineering, College of Engineering; University of California, Berkeley, California

ABSTRACT

Detailed electron metallographic studies are being made of interfacial dislocations which are formed to relieve the elastic coherency strains developed upon long aging of spinodal alloys in the systems Cu-Ni-Fe and Cu-Mn-Al. The stresses generated by the coherency strains are sufficiently large to exceed the yield strength of the alloys so that the interface dislocations can be generated by plastic deformation. These slip dislocations accommodate the lattice mismatch at the interphase interfaces. The geometry of the arrangements is determined by the operative slip systems, by the degree of long range order (if any) and by the requirement that the Burgers vector or a large component thereof also lies in the interface plane. The model proposed for the formation of the interface dislocations suggests that during coarsening, the two coherent spinodal phases experience tensile and compressive stresses producing dislocations which glide on slip planes from opposite interfaces and are then incorporated into the interface. As a consequence, the interface planes change their orientation and {100} habit is lost. In Cu-Ni-Fe {110} faces develop and this shape change is expected from the slip model, since in this alloy the dislocations are generated on {111} slip planes and their a/2 ⟨110⟩ Burgers vectors lie in a (001)

plane adjacent to the plane of the interface. Rearrangement of the dislocation structures at the interfaces may be accomplished by climb. In Cu-Mn-Aℓ the dislocations lie in the {001} interface and have ⟨100⟩ Burgers vectors. These can only develop from slip dislocations after combination reactions and climb.

1. INTRODUCTION

Although the kinetic and thermodynamic aspects of spinodal transformations are well established,[1-4] there are relatively few reports of detailed morphological studies {See e.g. (4)} except for recent papers on the Cu-Ni-Fe system[5,6] and a report of spinodal characteristics in ordered Heusler alloys.[7] Both phases in spinodal alloys have the same crystal structure but different compositions, but very little is known about the structure of the interface when coherency is lost. In a symmetrical fcc Cu-Ni-Fe alloy which decomposes along {100} planes, Butler and Thomas[5] reported the formation of a/2 ⟨110⟩ interface dislocations when the wavelength exceeded about 1000Å and also noted that the interface plane became irregular with a tendency to change orientation from {100} interfaces towards {110} interfaces. However the analyses did not permit a complete description to be made of the interface structure and it was suggested that the dislocations were spontaneously created at the interface. The present paper describes more detailed studies of the interface structures in Cu-Ni-Fe. The results are interpreted in terms of plastic deformation which occurs due to the stresses associated with the strains from lattice mismatch. This model is based on that developed earlier from diffusional studies in silicon,[8,9] although nucleation of the dislocations[5,10] has not been resolved. This paper also describes interfacial dislocations in the Heusler type alloy Cu-Mn-Al which also appears to undergo spinodal decomposition.[7]

2. EXPERIMENTAL PROCEDURE

2.1 Alloy Preparation and Heat Treatment

The alloys were prepared by melting the charges in a large induction furnace in an helium atmosphere. The compositions of the three alloys studied, in atomic percent, were:

alloy 1: 51.5 Cu - 33.5 Ni - 15.0 Fe

alloy 2: 64 Cu - 27 Ni - 9 Fe

alloy 3: 62.5 Cu - 12.5 Mn - 25 Al

To reduce segregation during solidification, the molten charges were chill cast into water cooled copper molds. X-ray fluorescent analysis verified to within ± 1% the compositions given above.

After a homogenization treatment at 1050°C for three days, the Cu-Ni-Fe ingots were initially hot worked and then cold rolled to a final thickness of 8 mils. These sheets were subsequently homogenized for 2 hours at 1050°C, quenched into ice brine and then aged at 775°C for times ranging from 100 hours to 840 hours.

The Cu-Mn-Al alloy was homogenized at 850°C for 72 hours. The ingot was then cut into discs 0.020 in. thick. The discs were aged at 300°C for times ranging from 30 sec. to 160 hours.

2.2 Electron Microscopy

Thin foils were prepared in the usual way and examined in the Siemens Elmiskop 1 microscope. using the appropriate diffraction and imaging techniques.[11] Weak beam images were occasionally studied in

order to remove Moiré interference fringes and to greatly improve resolution of dislocation images.[12] However this method is tedious and involves long exposures (20 sec.) and applies only to thin areas. High voltage electron microscopy was also used to take advantage of the improvement in resolution of lattice defects using strong beams systematic orientations[13] and the increased penetration that accompanies an increase in accelerating voltage.[14,15] The latter is advantageous in these alloys systems since one phase tends to be dissolved at a faster rate than the other (e.g. in Cu-Ni-Fe, the Cu rich phase). In addition to the usual contrast experiments needed to define Burgers vectors of dislocations, stereomicroscopy was done to assist in characterizing the three-dimensional geometries of interfaces.

3. EXPERIMENTAL RESULTS

3.1 Cu-Ni-Fe Alloys

These alloys are fcc and growth from the spinodal reaction produces a two phase structure with interface planes parallel to {100} planes.[5,6] Hence the expected interfacial dislocations should have ⟨100⟩ or ⟨110⟩ Burgers vectors. Preliminary results[5] showed that the Burgers vectors were of the ⟨110⟩ type but it was not ascertained whether the dislocations and their Burgers vectors both lay in the interface plane. Stereomicroscopy (Fig. 1) showed that the dislocation lines lie in the interface and are probably not prismatic loops[10,11] since oscillatory contrast is not observed.

Before dislocation contrast is resolved at the interface, the elastic strains maximize normal to the interface plane so inducing

local tetragonality which has been measured as 0.8% strain for these Cu-Ni-Fe alloys.[5] This tetragonality is relieved by the generation of the interface dislocations. Contrast experiments utilizing suitable foil orientations (See Table I) proved that the interfacial dislocations had a/2 ⟨110⟩ type Burger vectors. Typical contrast analyses are shown in Figs. 2,4,5,6. Trace analyses and contrast experiments showed that most of the Burgers vectors were inclined at 45° to the plane of the interface containing the dislocation and made an angle of either 60° or 45° with the dislocation line. For example, in the (111) slip plane the dislocation lines lie along $[\bar{1}10]$ in the (001) interface plane with Burgers vectors parallel to $[\bar{1}01]$ or $[0\bar{1}1]$, lying in (010) or (100). This geometry is expected if dislocations on {111} with 60° Burgers vectors slip to the interface until the lines lie in the interface but with their Burgers vectors lying out of this interface. The crystallographic geometry can be visualized using the (001) stereogram given in Fig. 3, and is described for each possible {001} interface in Table II. Similar geometries apply to the other {111} slip planes.

When the particles in the Cu-Ni-Fe alloys begin to lose coherency as evidenced by the appearance of dislocations at the interface, the particle morphology tends to become very irregular and the (100) interface plane is stepped and changes towards the (110) plane. This is well illustrated in Figs. 4,5. A shape change from (100) towards (110) would be expected if plastic deformation occurred with slip in ⟨110⟩ occurring from opposite interfaces.

Table I. Diffraction conditions for dislocation contrast ($\bar{g}\cdot\bar{b}$ products) in f.c.c. Cu-Ni-Fe alloys.

		Reflection ($\bar{g}$)										
		$11\bar{1}$	$02\bar{2}$	$\bar{1}1\bar{1}$	200	$13\bar{1}$	$\bar{1}3\bar{1}$	$11\bar{1}$	$3\bar{1}\bar{1}$	$\bar{2}20$	$31\bar{1}$	$13\bar{1}$
Direction of Burgers vector ($\bar{b}$)	[100]	X	0	X	X	X	X	X	X	X	X	X
	[010]	X	X	X	0	X	X	X	X	X	X	X
	[001]	X	X	X	0	X	X	X	X	0	X	X
	[110]	X	X	0	X	X	X	X	X	0	X	X
	[$\bar{1}$10]	0	X	X	X	X	X	0	X	X	X	X
	[101]	0	X	X	X	0	X	0	X	X	X	0
	[$\bar{1}$01]	X	X	0	X	X	0	X	X	X	X	X
	[011]	0	0	0	0	X	X	0	X	X	0	X
	[0$\bar{1}$1]	X	X	X	0	X	X	X	0	X	X	X

(011) zone (013) zone (112) zone (114) zone

For $\bar{g}\cdot\bar{b}$ = 0 dislocations will be out of contrast.

For $\bar{g}\cdot\bar{b}$ = X dislocations will be out of contrast.

XBL 718-7174

Table II. Slip systems expected to be activated in fcc structures, for normal stresses in ⟨ 001 ⟩ .

Stress axis (σ)	Interface plane $\perp$ to σ	Slip planes	Expected Burgers vectors ($\bar{b}$)	Interface planes containing $\bar{b}$
[001]	(001)	(111)	$[\bar{1}01]$, $[0\bar{1}1]$	(010) (100)
		$(\bar{1}11)$	[101], $[0\bar{1}1]$	(010) (100)
		$(\bar{1}\bar{1}1)$	[101], [011]	(010) (100)
		$(1\bar{1}1)$	$[\bar{1}01]$, [011]	(010) (100)
[100]	(100)	(111)	$[1\bar{1}0]$, $[\bar{1}01]$	(001) (010)
		$(\bar{1}11)$	[110], [101]	(001) (010)
		$(\bar{1}\bar{1}1)$	$[1\bar{1}0]$, [101]	(001) (010)
		$(1\bar{1}1)$	[110], $[\bar{1}01]$	(001) (010)
[010]	(010)	(111)	$[\bar{1}10]$, $[0\bar{1}1]$	(001) (100)
		$(\bar{1}11)$	[110], $[0\bar{1}1]$	(001) (100)
		$(\bar{1}\bar{1}1)$	$[\bar{1}10]$, [011]	(001) (100)
		$(1\bar{1}1)$	[110], [011]	(001) (100)

XBL 718-7176

At some of the interfaces, the dislocations appear to be rotating such that the dislocation lines lie along [100] (See Figs. 2,6) and in areas where the rotated sets of dislocations intersect the first set, the dislocation lines are jogged. The examination of thicker foils in the high voltage electron microscope revealed the presence of large tangles of "stray" dislocations some of which do not lie in the interface (e.g. Fig. 7). This result indicates that plastic deformation (creep) has occurred during aging.

3.2 Heusler Type Cu-Mn-Al Alloy

The alloy studied here has a composition half way between Cu_2 Mn Al and Cu_3 Al and upon quench-aging possesses all the metallographic characteristics of a spinodal decomposition,[7] e.g. Fig. 8(a). The diffraction pattern of a fully decomposed alloy can be indexed in terms of the unit cells of the ordered structures of Cu_2 Mn Al and Cu_3Al. The ternary constituent has the $L2_1$ structure and the binary constituent has the closely related DO_3 structure. Their lattice parameters differ by 2%. This value compares with that calculated from diffraction patterns and Moiré images from a fully aged alloy (1.6% ± 0.5%). Before the coherency between the two phases is lost, the diffraction pattern shows streaking of all reflections in ⟨100⟩ directions normal to the longest dimensions of the particles (Fig. 8). It was observed that the streaks are formed by two intensity maxima which produce complementary dark field images. Furthermore, the spacing between the intensity maxima increases with the order of the reflection. This can be explained by a small tetragonality of the two phases. The

presence of the streak through the transmitted beam can be explained by double diffraction in the elastically strained thin foil.

Upon further aging and similarly to Cu-Ni-Fe, the Cu-Mn-Al alloys lose coherency when the wavelengths exceed 1000Å and the coherency strains are relieved by the formation of interfacial dislocations. Contrast experiments have shown that the dislocations are pure edge dislocations and that their Burgers vectors are in ⟨100⟩, lying in the plane of the interface. One such experiment is shown in Fig. 9 [See also Table III]. It can also be seen that the interface is smoothly curved around the particles. In addition the accompanying diffraction pattern shows that the lattice parameter difference, as reflected by the difference in reciprocal lattice vector lengths (Δg), associated with each reflection is in a direction always parallel to g. This suggests that in the fully aged condition, the two phases have returned to their cubic symmetry. This behavior is similar to that found in the Cu-Ni-Fe alloys.

The interface can also be imaged by Moiré fringe interference. With this type of contrast which can sometimes obscure the dislocation contrast at the interface, it is difficult to compare various dislocation images in order to determine the Burgers vectors of the dislocations. The weak beam image[12] was found to improve the contrast of the dislocation images by decreasing the Moiré fringe interference and also by decreasing the width of the dislocation line. This is shown in Fig. 10. Both Figs. 10(a) and (b) were obtained using the 242 reflection but in (a) the Kikuchi line was passing through the

Table III. Diffraction conditions for dislocation contrast in Cu_2 Mn Al having the $L2_1$ structure.

		Reflection ($\bar{g}$)				
		200	020	220	242	$\bar{2}42$
Direction of Burgers Vector ($\bar{b}$)	⟨111⟩	X	X	X	X	0
	⟨11$\bar{1}$⟩	X	X	X	0	X
	⟨1$\bar{1}$1⟩	X	X	0	X	X
	⟨$\bar{1}$11⟩	X	X	0	0	X
	⟨100⟩	X	0	X	X	X
	⟨010⟩	0	X	0	X	X
	⟨001⟩	0	0	0	X	X

All indices refer to the lattice parameter of the ordered unit cell which is twice the lattice parameter of the disordered unit cell.

XBL 718-7175

operating reflection whereas in (b) the foil was slightly tilted so that the Kikuchi line passes at the 1/2g position.

3.3 Summary of Results

The Cu-Ni-Fe alloys develop dislocation structures consisting of dislocations lying in {001} with a/2 ⟨ 011 ⟩ slip Burgers vectors inclined at 45° to the plane of the interface containing the lines. The Cu-Mn-Al alloy developes interface dislocations lying in pure edge orientation in the {001} interface planes and with ⟨ 100 ⟩ Burgers vectors.

4. DISCUSSION

4.1 Proposed Model For Loss of Coherency in Cu-Ni-Fe Alloys

The experimental observations for the fcc Cu-Ni-Fe alloys indicate that the interface dislocations originate as slip dislocations and that the final dislocation networks are produced by the climb of these dislocations in the interface. The interface dislocations have Burgers vectors of the type a/2 ⟨ 110 ⟩ rather than the expected $\bar{b}$ = a ⟨ 100 ⟩ which would give the minimum energy for the interfacial dislocation network. Also, the fact that the Burgers vectors do not lie in the {001} interface planes containing the dislocation lines suggests that shear stresses arising from the coherency strains normal to the interfaces may generate slip dislocations. Other observations that suggest a slip dislocation model for explaining the results are 1) that some of the dislocations lie along ⟨ 110 ⟩ directions which

are the lines of intersection of {111} slip planes and {001} interface planes 2) that the interface planes tend to change from {001} to {011} during growth, 3) in thick foils non-interface dislocations can be resolved.

The proposed model for the loss of coherency is based on the generation of slip dislocations that may either remain at the interface where created or more likely glide across the particle to the opposite interface. Obviously such glide will involve dislocation generation from opposite interfaces. For the purpose of analysis the physical situation will be idealized as one dimensional platelets, infinite in extent, with coherency strains acting normal to the interfaces. The actual particle morphology of course is much more complex than this simple model. It is important to remember that one of the phases is in compression (i.e. Cu-rich) and the other in tension since the sense of the stress determines the relative orientation of the Burgers vectors with respect to the interface. The details of the model are as follows.

The coherency strains at the interface can be relieved by the generation of slip dislocations on favorably oriented slip systems for which the resolved shear stress or Schmid factor (m) is greatest viz.

$$m = \cos \phi \cos \lambda$$

where ϕ is the angle between the slip plane normal and the stress axis (which is normal to the interface plane) and λ is the angle between the slip direction and the stress axis. The nucleation of the dislocation loops has not yet been observed directly so the mechanism of

origin is not known. They could be formed spontaneously as discussed earlier[5] or from the accumulation of excess vacancies.[16]

The strain as estimated from the lattice spacing differences measured from diffraction patterns are 0.8% for Cu-Ni-Fe and 1.6% for Cu-Mn-Al. Assuming Hooke's law, the corresponding stress for Cu-Ni-Fe is 0.008 × Young's modulus (E) which is approximately $0.008 \times 3 \times 10^4$ kg/mm^2 ~ 200 kg/mm^2. This estimated coherency stress is much larger than the measured yield stress of 25 kg/mm^2 for alloy 1 aged at 775°C.[5] Previous work[8-10] regarding the accommodation of coherency strains by slip dislocations support the above arguments in that if the coherency strains are of the order of 0.1 to 1.0% then slip dislocations are favored to accommodate the lattice mismatch rather than the direct generation of interface dislocations. Because of the larger volume fraction and interface area of the minor phase in these spinodal Cu-Ni-Fe alloys, it is necessary that slip dislocations be generated to completely relieve the coherency strains.

The operative slip systems in Cu-Ni-Fe alloys are of the type {111}⟨011⟩. The specific slip systems that will be activated by the coherency stress normal to the interface are those for which the resolved shear stress is greatest (Table II). For example, the stereogram of a (001) projection given in Fig. 3 shows the relative orientation of the four {111} slip planes and the four possible a/2 ⟨110⟩ Burgers vectors that are expected to be activated by stresses along [001]. Because both positive and negative dislocations are two

distinct cases with respect to the tensile/compressive nature of the stress acting at the interface, there is a total of eight unique Burgers vectors that are associated with any given {001} interface. That is, if the compressive stress acting in the Cu-rich phase generates the slip dislocations then the resulting Burgers vectors will all lie on the same side of the interface; and conversely if the tensile stress acting in the Fe rich phase creates the dislocations then the Burgers vectors will lie on the opposite side of the interface. But it should be noted that if dislocations are generated at one interface and slip on {111} across the particle to the opposite interface, then it is possible to produce Burgers vectors that have the opposite sense relative to this interface. Actually it is most probable that slip occurs in only one phase (the softer Cu-rich phase) with dislocations moving in opposite directions from opposite interfaces. Such slip will produce the observed shape changes of the particles (Figs. 4-6).

A specific example illustrates the proposed dislocation mechanism for the loss of coherency. Consider the electron micrographs shown in Fig. 2. The two sets of dislocations that are shown lie in the (001) interface plane; and the dislocations that are in contrast in Fig. 2a have Burgers vector $a/2\ [\bar{1}01]$ whereas the dislocations visible in Fig. 2b have $\vec{b} = a/2\ [011]$ or $a/2\ [0\bar{1}1]$ and lie parallel to the [100] direction. Note that for both sets of dislocations the Burgers vectors do not lie in the interface but are

inclined at 45° to it. If one assumes that the two Burgers vectors lie on opposite sides of the interface and takes for the second set of dislocations $\bar{b} = a/2\,[01\bar{1}]$, then the vectorial sum is:

$$a/2\,[\bar{1}01] + a/2\,[01\bar{1}] = a/2\,[\bar{1}10]$$

This resultant displacement lies in the (001) interface plane and completely relieves the lattice mismatch in this plane. But if both Burgers vectors lie on the same side of the interface, then the resultant displacement does not lie in the interface and is given by the vectorial sum:

$$a/2\,[\bar{1}01] + a/2\,[0\bar{1}1] = a/2\,[\bar{1}\bar{1}2]$$

This displacement relieves the lattice mismatch in the interface with an additional component normal to it.

The dislocations shown in Fig. 2a lie along the directions [010], [110] and [$\bar{1}$10]. Now [110] and [$\bar{1}$10] are the lines of intersection of the ($\bar{1}$11) and ($\bar{1}\bar{1}$1) slip planes respectively with the (001) plane. Some of the dislocations that lie along [110] appear to be changing direction towards [010]. Because the lattice mismatch at the interface is accommodated by the resolved edge component of the dislocation in the direction of mismatch, one would expect this rotation to occur so that the dislocation lines with $\bar{b} = a/2\,[\bar{1}01]$ would be so oriented as to relieve the lattice mismatch in the [100] direction. Such motion must occur by climb.

To summarize the main points of this model for the loss of coherency, it is proposed that slip dislocations are generated at the interfaces and either remain at the interface where created or else glide across the particle to the opposite interface. For the two- or three-dimensional case (i.e. rods or cubes), the dislocations could possibly move to adjacent {001} interfaces. Then by a subsequent climb process the dislocation lines rotate in the interface such that they lie along ⟨100⟩ directions so as to accommodate the lattice mismatch in the interface.

Support for this model comes from earlier work on the diffusion gradients and interfaces generated by phosphorus and boron solute diffusion in silicon.[8,9] In the latter system it was shown that the stresses developed at the maximum gradient produced glide dislocations on those slip systems of maximum Schmid factor. Thus different geometries of dislocations resulted by choosing different orientations for the diffusion.

4.2 The Cu-Mn-Al Alloy

Since the interface dislocations in this alloy are {001} ⟨001⟩ type they cannot be produced directly by slip, since there is zero shear stress on {001} ⟨001⟩ for tensile/compressive stresses normal to the interface planes {001}. However the resolved shear stress is very favorable for slip on the {011} ⟨111⟩ or {011} ⟨01$\bar{1}$⟩ systems expected for this alloy (See Fig. 3).

However if dislocations are generated by glide, in order to produce the observed ⟨ 001 ⟩ dislocations there must be combination reactions in the {011} slip planes. For example, if we consider the coherency stress in [001] then the following reactions involving dislocations moving from opposite interfaces can produce the required interface dislocations:

Interface Plane	Stress Axis	Slip plane	Burger vectors and reactions
		[101]	$a/2[\bar{1}11]_+ + a/2[11\bar{1}]_- \rightarrow a[010]$
(001)	[001]	[$\bar{1}$01]	$a/2[111]_+ + a/2[\bar{1}1\bar{1}]_- \rightarrow a[010]$
		[011]	$a/2[1\bar{1}1]_+ + a/2[11\bar{1}]_- \rightarrow a[100]$
		[01$\bar{1}$]	$a/2[111]_+ + a/2[1\bar{1}\bar{1}]_- \rightarrow a[100]$

The + and - signs indicate the sense of glide on the slip planes.

It is also possible that slip systems of the {110} ⟨ 110 ⟩ type operate. Strutt and Row[18] indicate that such glide occur in Ni_2(Al Nb) which also possesses the $L2_1$ structure. It is therefore possible to predict the following dislocation reactions required to give the interface dislocations. For the (001) interface, the slip system are (011) [0$\bar{1}$1], (0$\bar{1}$1)[011], ($\bar{1}$01)[101] and (101) [10$\bar{1}$] and their negatives. Thus reactions such as

$$a/2[0\bar{1}1] + a/2[0\bar{1}\bar{1}] \rightarrow a[0\bar{1}0]$$
$$\text{in } (011) \quad \text{in } (0\bar{1}1) \quad \text{in } (001)$$

can account for the observed {001} ⟨ 001 ⟩ dislocations. It is not known which of the above mechanisms is the most probable. These

reactions produce the required Burgers vector but the resultant line must climb to the respective interface plane.

A further restriction in the Cu-Mn-Al spinodal alloys is that both phases are ordered. Thus it is likely that slip procedes by the motion of superlattice dislocation pairs of a/4 ⟨ 111 ⟩ Burgers vector. In this case one expects to find the interface dislocation also to be superlattice pairs of Burgers vectors a/2 ⟨ 100 ⟩. However within the resolution limits of the present techniques viz ~ 50Å for dislocations, using many beams at high voltages, we do not resolve dislocation pairs at the interface. Although there are many more restrictions on the slip model in Cu-Mn-Al than in Cu-Ni-Fe alloys it is reasonable to expect plastic deformation to occur due to the large coherency strains developed during growth. If the model is correct for Cu-Mn-Al it is anticipated that ⟨ 111 ⟩ dislocations might be resolved during the initial stages of coherency breakdown. Experiments are now in progress to check this.

ACKNOWLEDGEMENTS

One of us, M. Bouchard acknowledges receipt of a research fellowship from Hydro-Quebec, Montreal Canada. This work was done under the auspices of the United States Atomic Energy Commission.

REFERENCES

1. J. W. Cahn, Trans. TMS-AIME 242, 166 (1968).
2. J. W. Cahn Acta Met., 14, 1685 (1966).
3. J. E. Hilliard, "Spinodal Decomposition" in Phase Transformations, p. 497, Amer. Soc. for Metals, Metals Park, Ohio (1970).
4. D. de Fontaine, "Development of Fine Coherent Precipitate Morphologies by the Spinodal Mechanism" in Ultrafine-Grain Metals, p. 93, Syracuse Univ. Press, Syracuse, N.Y. (1970).
5. E. P. Butler and G. Thomas, Acta. Met. 18, 347 (1970).
6. R. J. Livak and G. Thomas, Acta Met. 19, 497 (1971).
7. M. Bouchard and G. Thomas, Proceedings of 29th Annual Electron Microscopy Society of America Meeting, p. 126, Claitor's Publishing Div., Baton Rouge, La. (1971).
8. J. Washburn, G. Thomas, and H. J. Queisser, J. Appl. Phys. 35, No. 6, 1909 (1964).
9. E. Levine, J. Washburn and G. Thomas, J. Appl. Phys. 38,No. 81, 87 (1967).
10. G. C. Weatherly and R. B. Nicholson, Phil. Mag. 17, 801 (1968).
11. G. Thomas, "Modern Diffraction and Imaging Techniques in Materials Science" (Eds. Amelinckx et. al) p. 131, North Holland (1970).
12. D. J. H. Cockayne, I. L. F. Ray and M. J. Whelan, Phil. Mag. 20, 1265 (1969).
13. R. Osiecki and G. Thomas, see ref. 7, p. 178.
14. G. Thomas Phil. Mag. 17, 1097 (1968).

15. V. E. Cosslett, see ref. 11, p. 341.

16. R. G. Baker, D. G. Brandon and J. Nutting, Phil. Mag., 4, 1339 (1959)

17. J. P. Hirth and J. Lothe, Theory of Dislocations p. 763, McGraw-Hill, New York (1968).

18. P. R. Strutt and G. M. Rowe, see ref. 7, p. 116.

FIGURE CAPTIONS

Fig. 1. Stereo micrographs taken of Cu-Ni-Fe (alloy 1) aged for 200 hours at 775°C showing the dislocations lying in the interface. Note: To obtain a stereo image, stereo glasses should be placed approximately 6 in. above and centered on the micrographs. The glasses may then be slightly rotated until the two black dots and the dislocation images are superimposed.

Fig. 2. Micrographs taken of the same area under different diffraction conditions in a Cu-Ni-Fe sample (alloy 2) aged for 200 hours at 775°C. The foil orientation was [013] zone axis; and thus the interfaces in which the dislocations lie are near the (001) plane. The dislocations visible in (a) have Burgers vector $a/2[\bar{1}01]$, whereas the dislocations seen in (b) have Burgers vectors $a/2[011]$ or $a/2[0\bar{1}1]$. Note that some of the dislocations in (a) lying along $[1\bar{1}0]$ appear to be rotating towards the [010] direction (see arrow).

Fig. 3. Standard (001) stereographic projection illustrating the relative geometry of the slip planes and Burgers vectors that are expected to be activated by coherency stress along [001].

Fig. 4. Micrograph taken of Cu-Ni-Fe (alloy 2) aged for 200 hours at 775°C showing stepped particle interfaces that may have resulted from dislocations gliding to the interfaces. Note that the interfaces tend to lie along {110} planes.

Fig. 5. Micrographs taken of the same area under different diffraction conditions for Cu-Ni-Fe (alloy 1) aged for 100 hours at 775°C showing two sets of dislocations. Note that on the stepped particle to the right the alternating groups of dislocations are in and out of contrast in (a) and (b). The foil orientation is [011] zone axis and the possible Burgers vectors in (a) are $a/2[\bar{1}10]$ or $a/2[101]$ and in (b) are $a/2[110]$ or $a/2[\bar{1}01]$.

Fig. 6. Micrographs taken of the same area under different diffraction conditions for Cu-Ni-Fe (alloy 2) aged for 200 hours at 775°C. The dislocations visible in (a) have $\vec{b} = a/2[110]$ or $a/2[\bar{1}01]$ whereas those visible in (b) and (c) have $\vec{b} = a/2[0\bar{1}1]$. Note that the dislocations visible in (b) and (c) appear to be rotating so that they lie along [100]. Notice a tendency for pairing of the second set of dislocations; these pairs are not dipoles as shown by the reversal of $\vec{g}$ from (b) to (c).

Fig. 7. High voltage electron micrograph taken using 500 kV accelerating voltage of Cu-Ni-Fe (alloy 1) aged for 200 hours at 775°C showing large tangles of dislocations some of which do not lie in the interfaces. Note that the narrow dislocation image width (~ 50Å) is characteristic of high voltage micrographs taken in a systematic orientation.

Fig. 8. Bright field micrograph showing the coherent spinodal in [010] and the corresponding diffraction pattern of the alloy $Cu_{2.5}Mn_{0.5}Al$ aged at 300°C for 1400 min. The diffraction pattern shows streaking in the cube direction normal to the longest dimension of the particles.

Fig. 9. Bright field micrographs of the same area and the corresponding diffraction pattern of the alloy $Cu_{2.5}Mn_{0.5}Al$ aged at 300°C for 10,000 min. This figures show the a/2 ⟨100⟩ type interfacial dislocations. The diffraction pattern reveals that the Δg is always parallel to g.

Fig. 10. Two dark field micrographs obtained by using the 242 reflection in the alloy $Cu_{2.5}Mn_{0.5}Al$ aged at 300°C for 10,000 min. In (a), the foil was oriented in the normal two beam condition and Moiré fringes are observed. In (b), the foil was oriented in a weak beam condition and the dislocation contrast is observed.

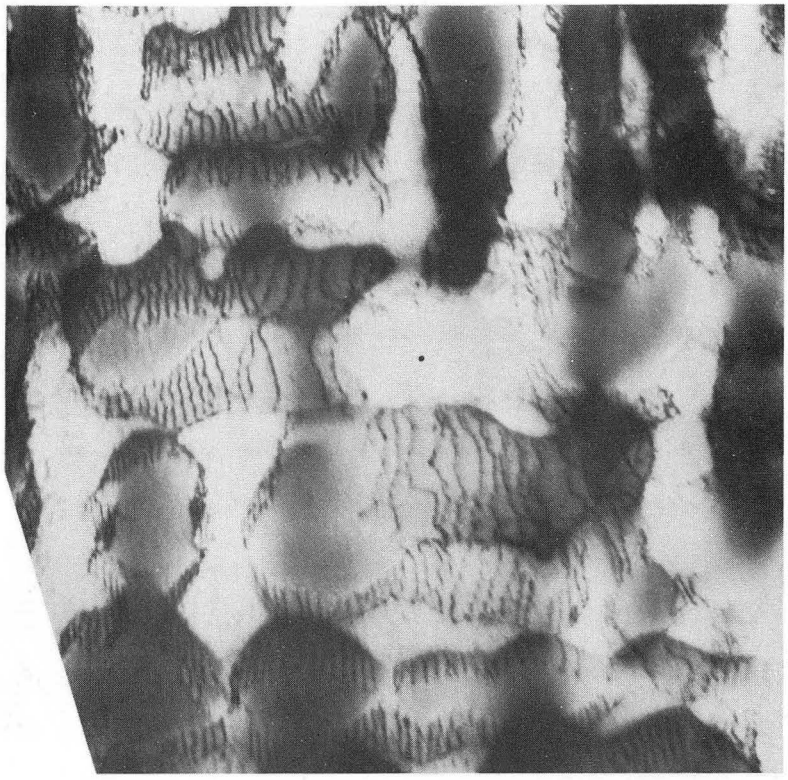

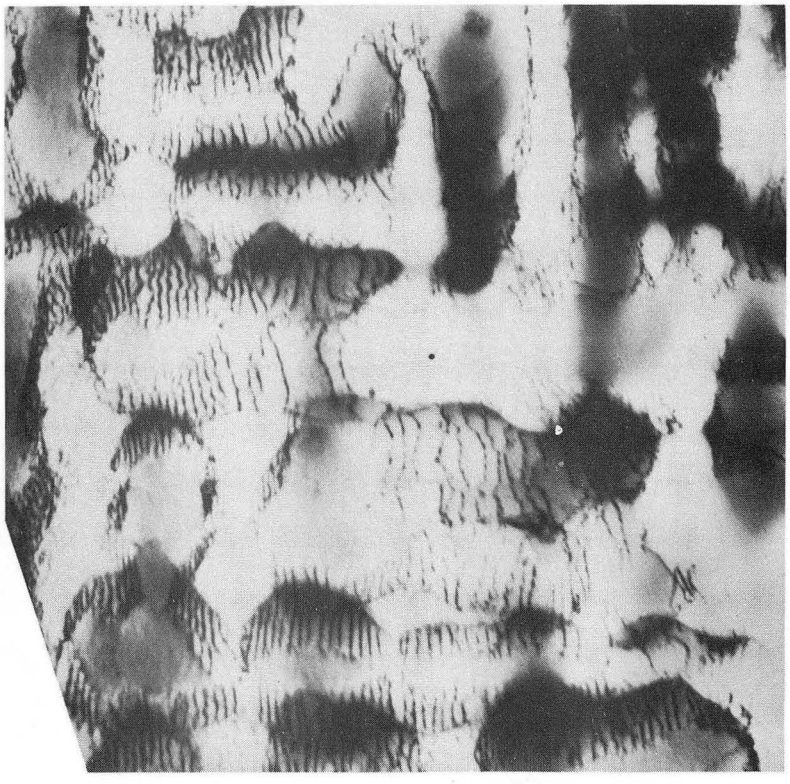

XBB 718-3798

Fig. 1

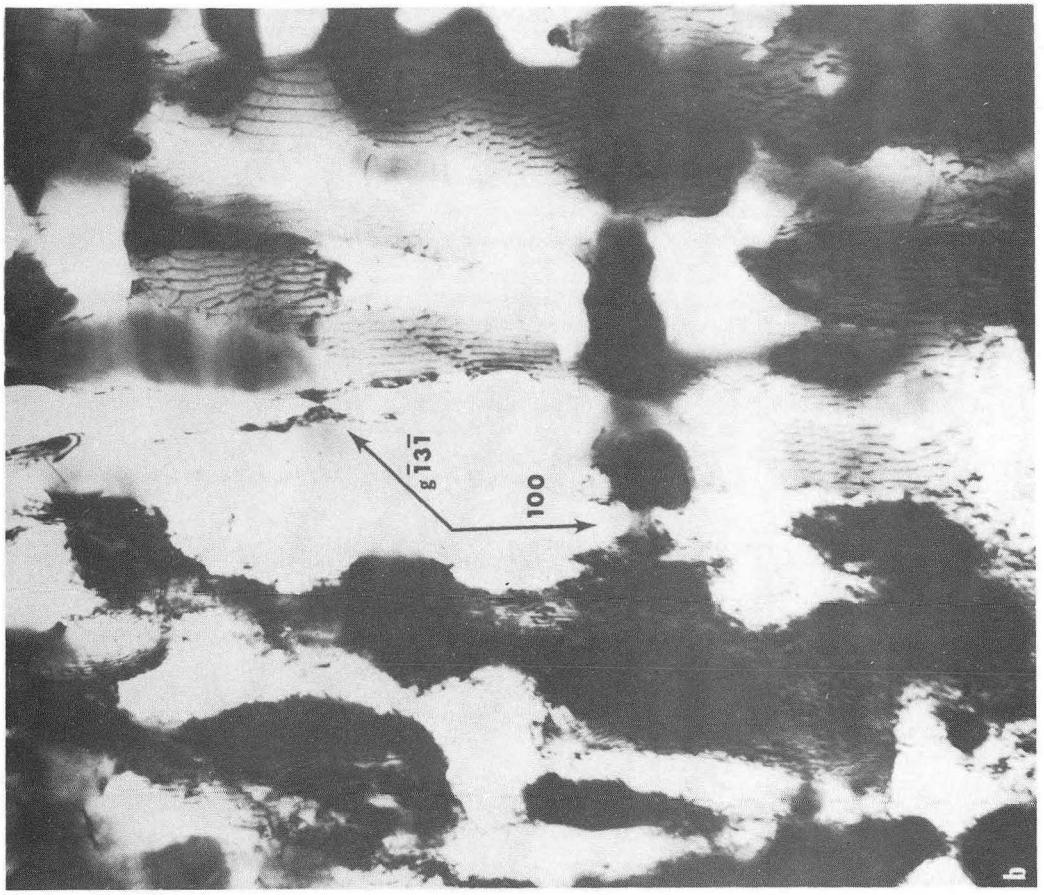

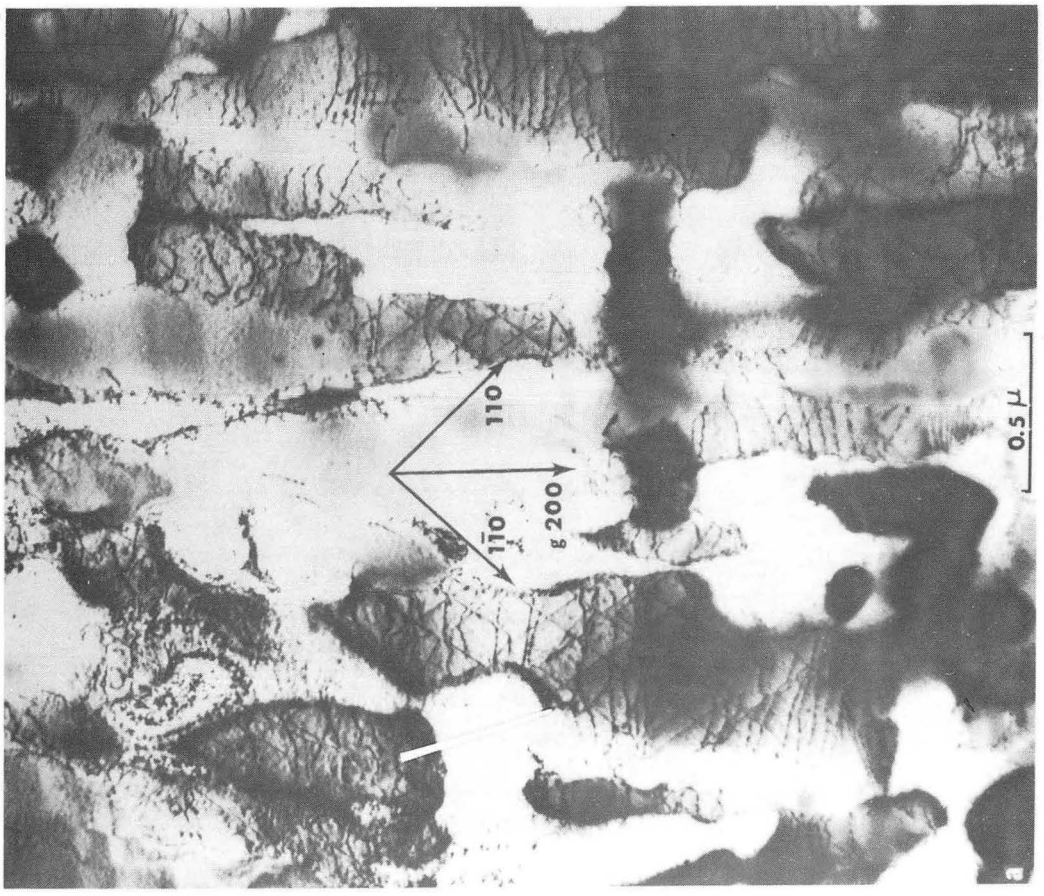

XBB 718-3732

Fig. 2

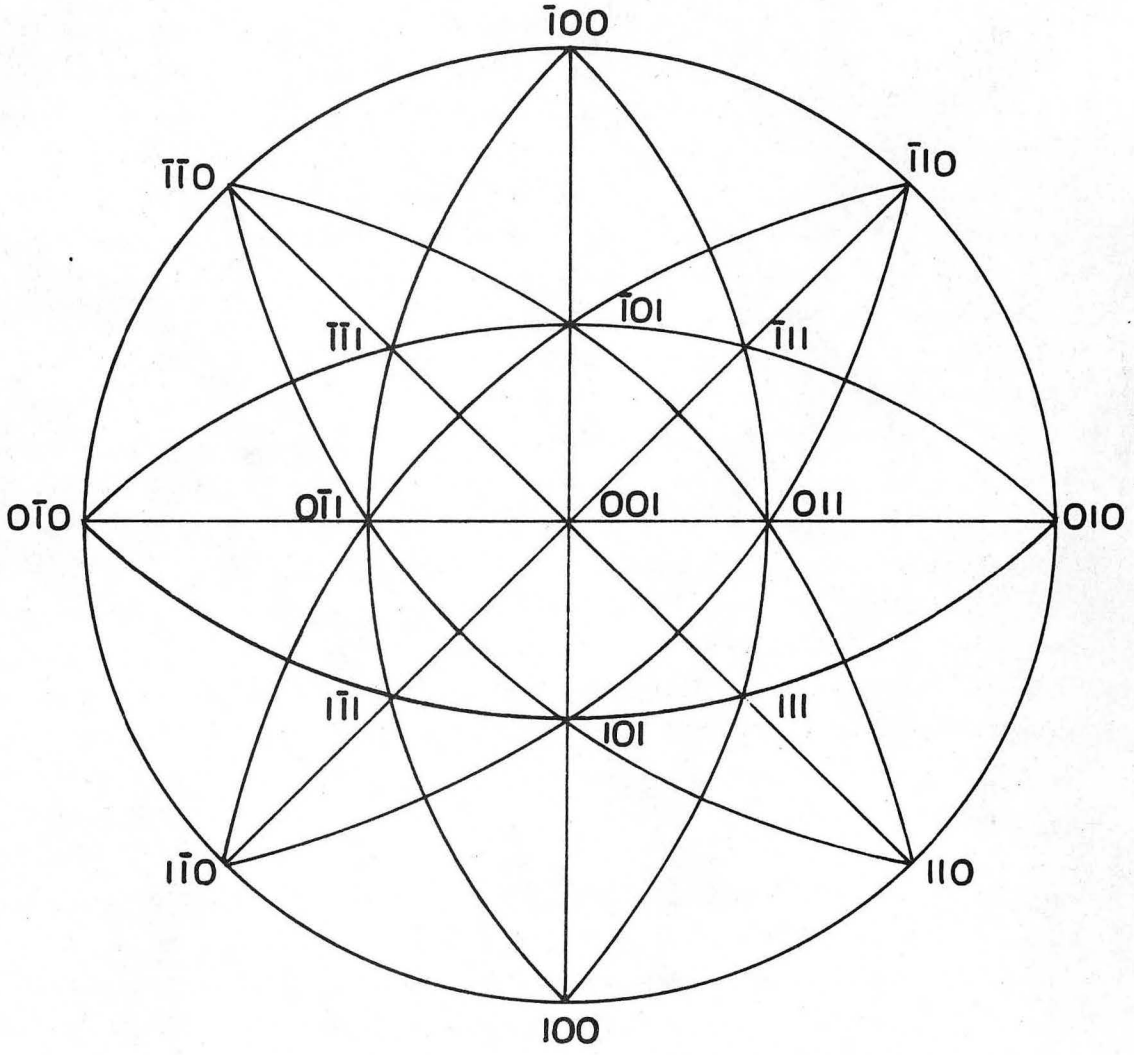

XBL 718-7192

Fig. 3

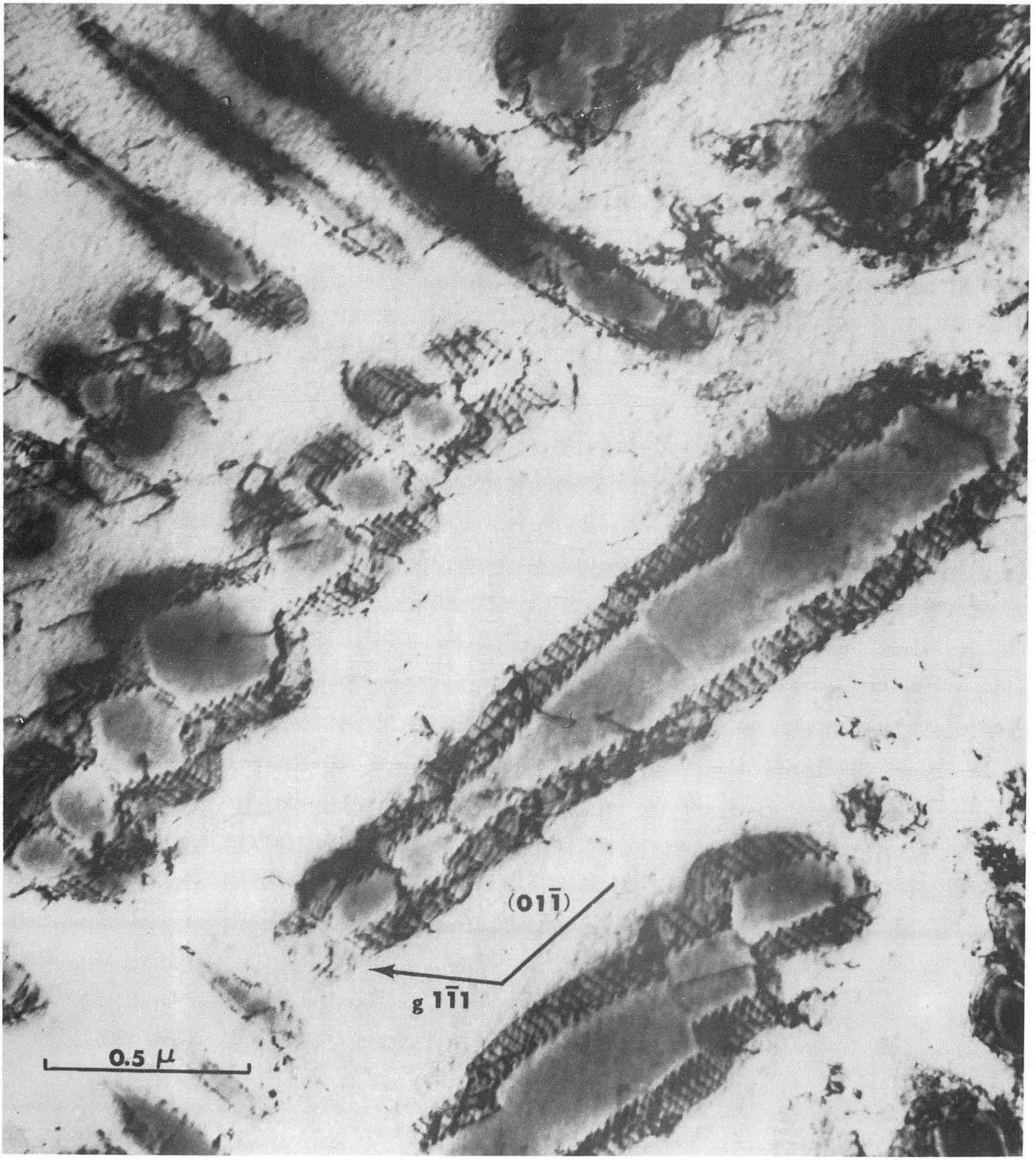

XBB 718-3730

Fig. 4

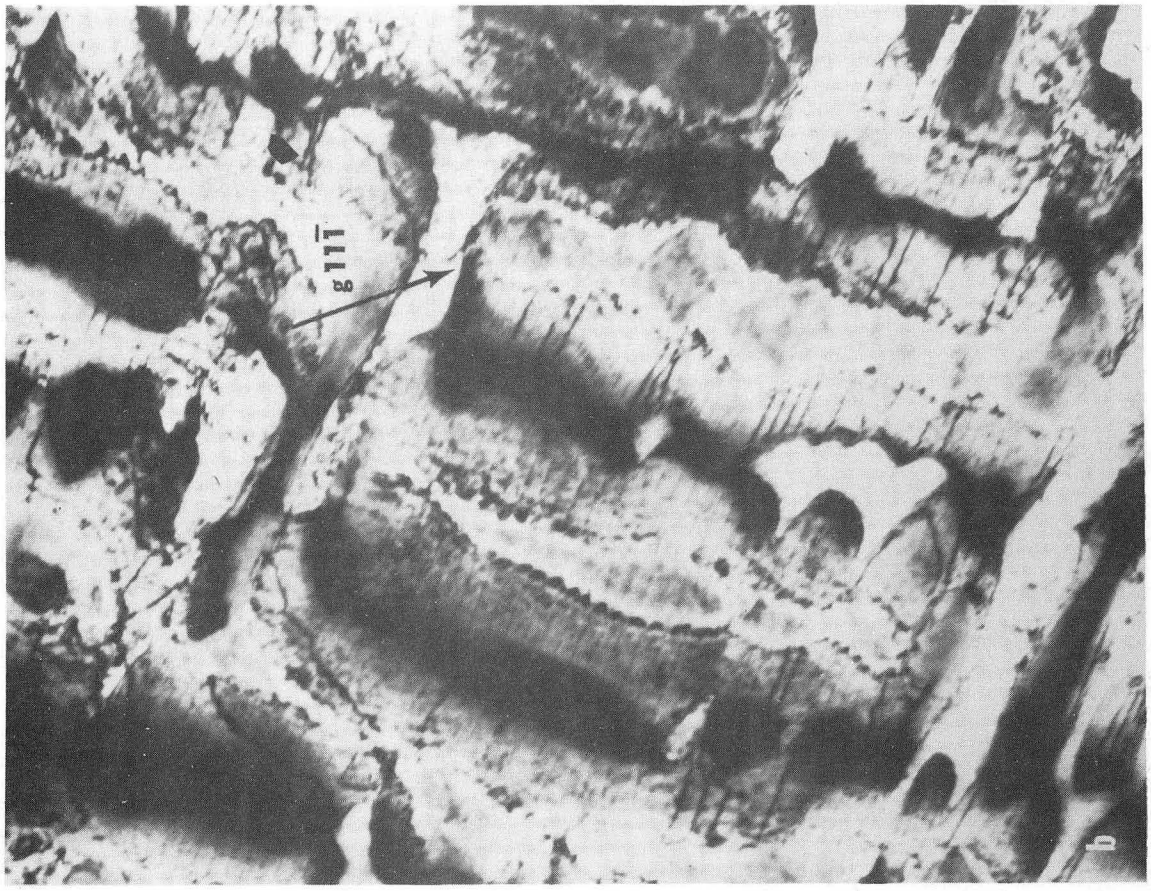

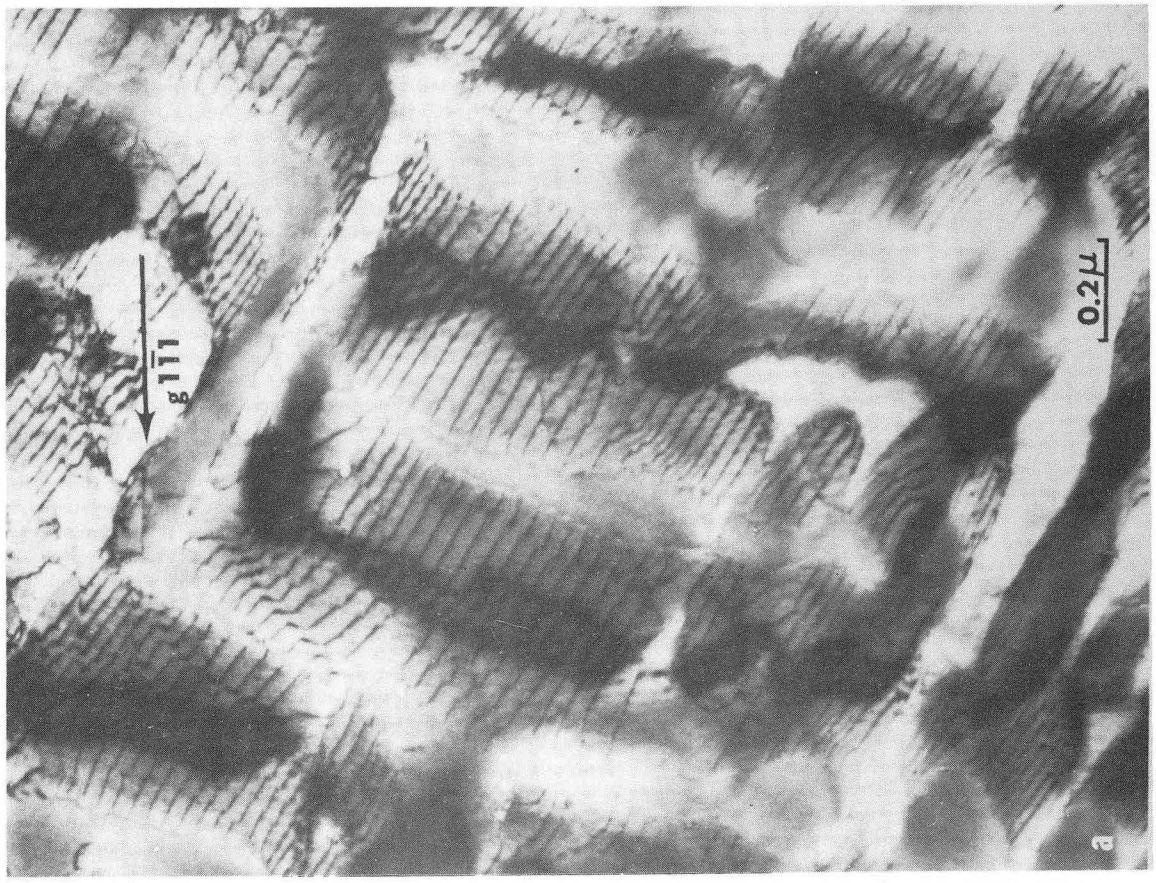

XBB 718-3733

Fig. 5

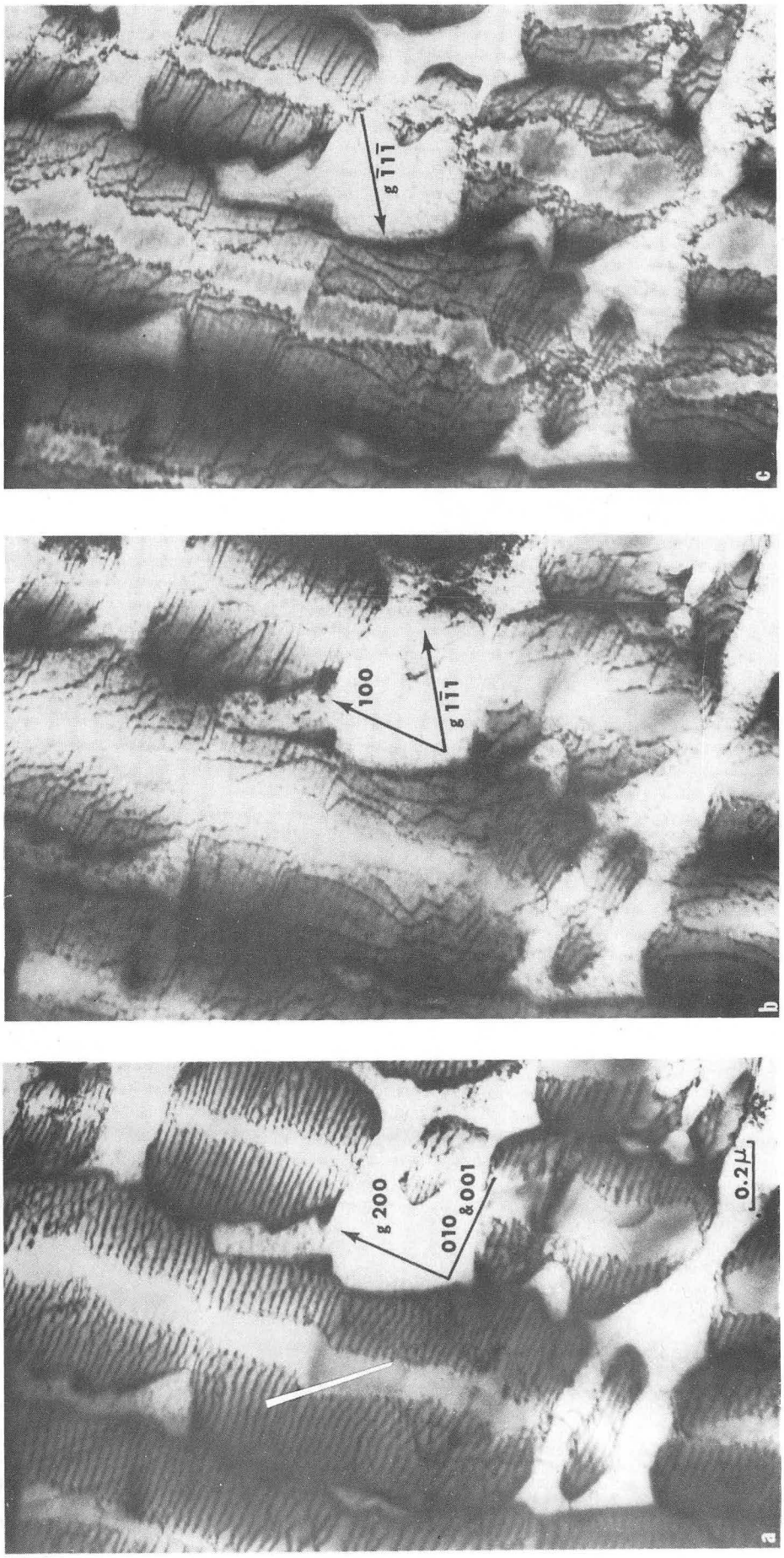

XBB 718-3729

Fig. 6

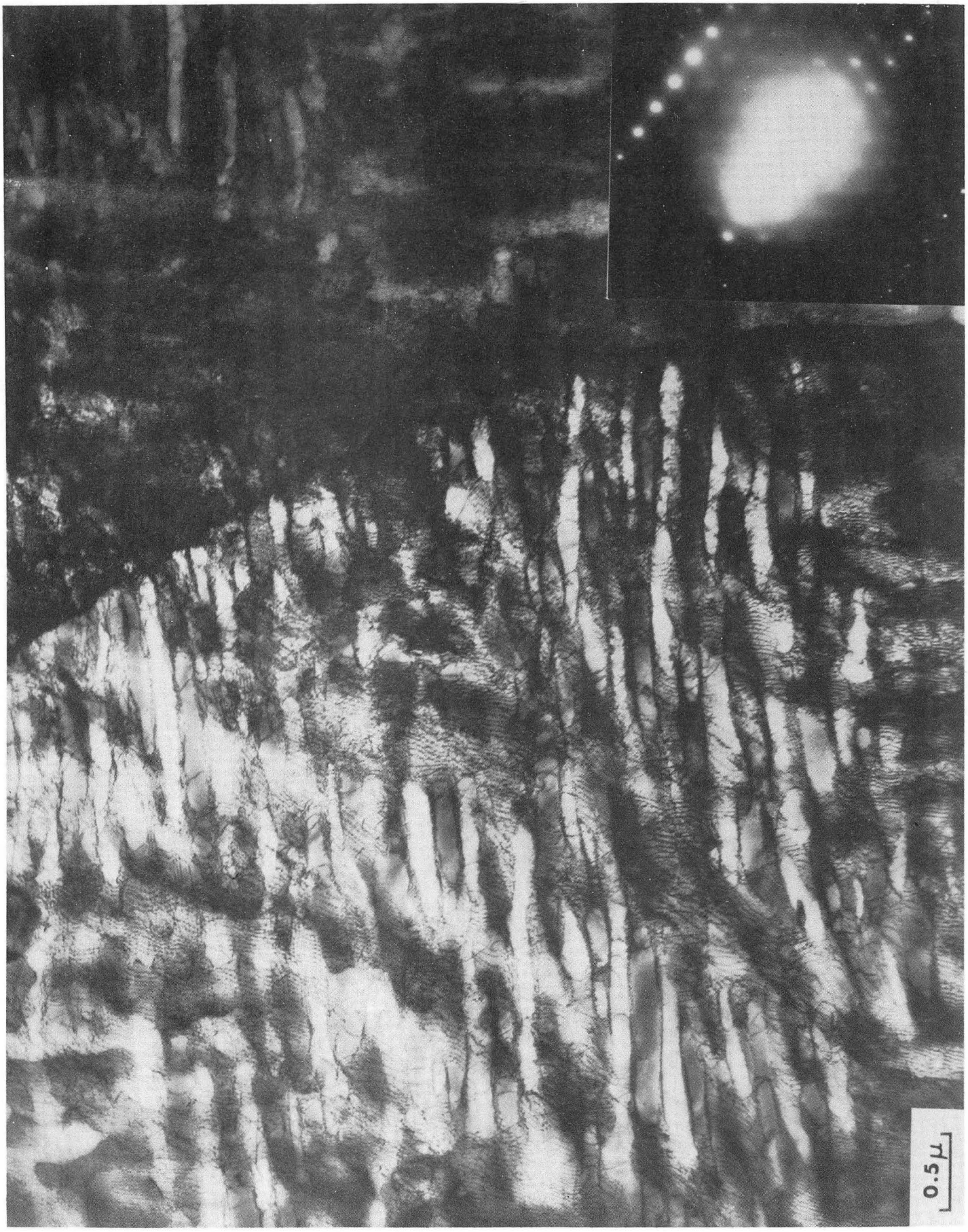

XBB 718-3728

Fig. 7

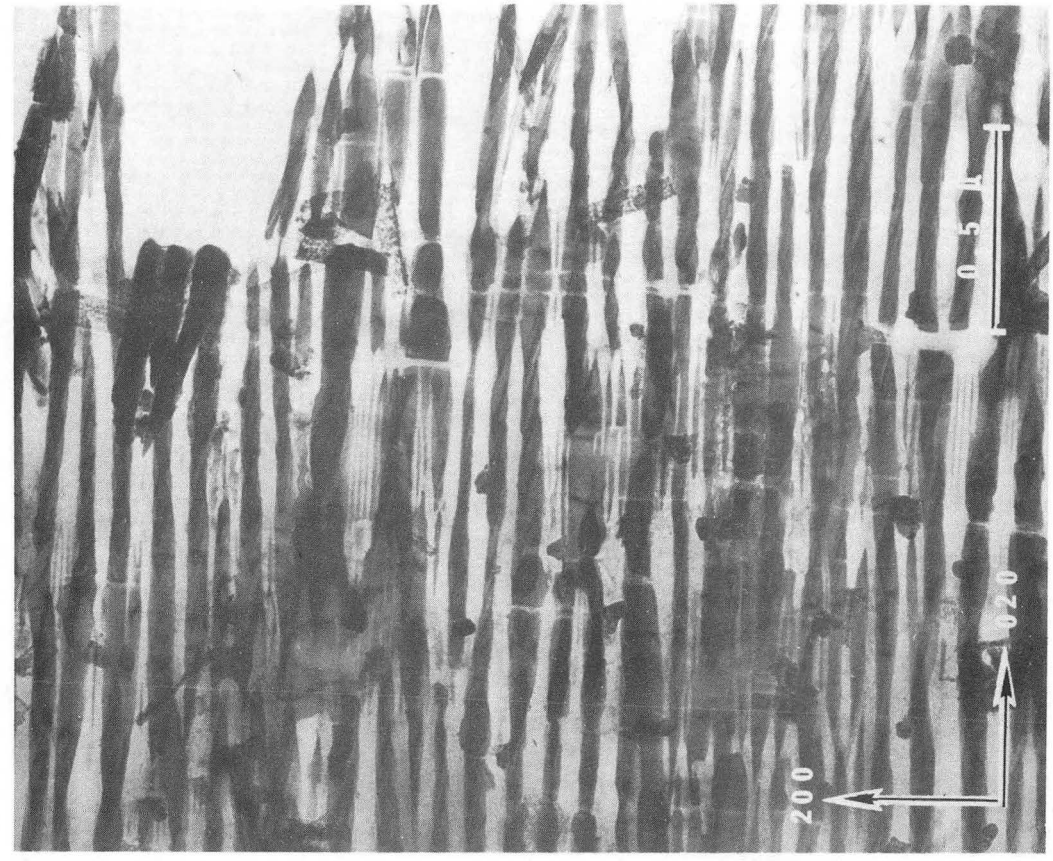

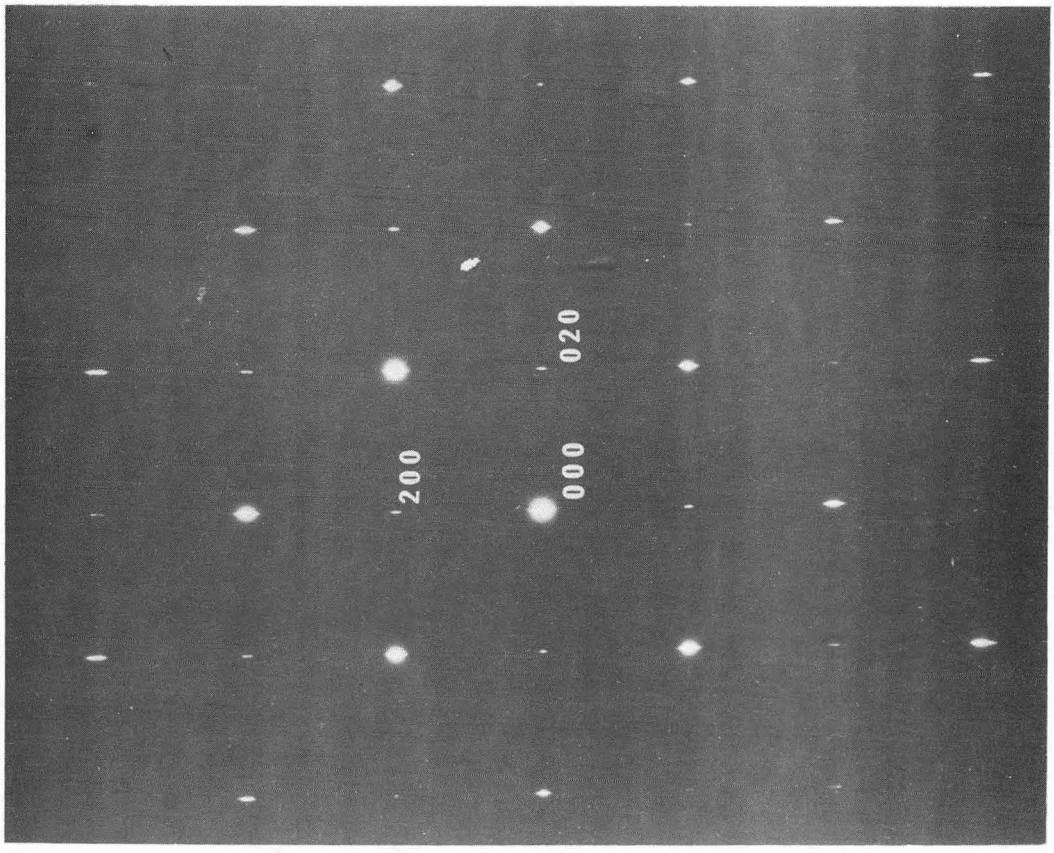

XBB 718-3542

Fig. 8

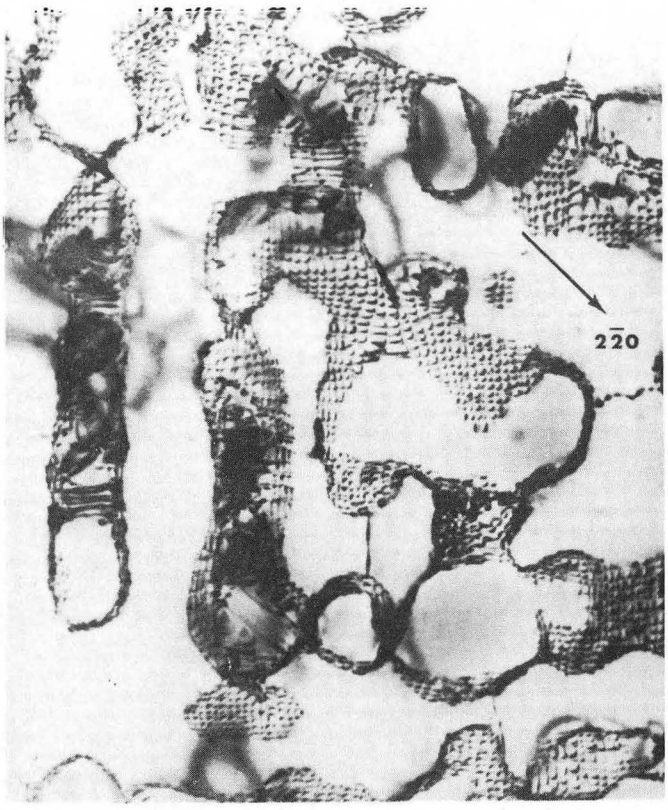

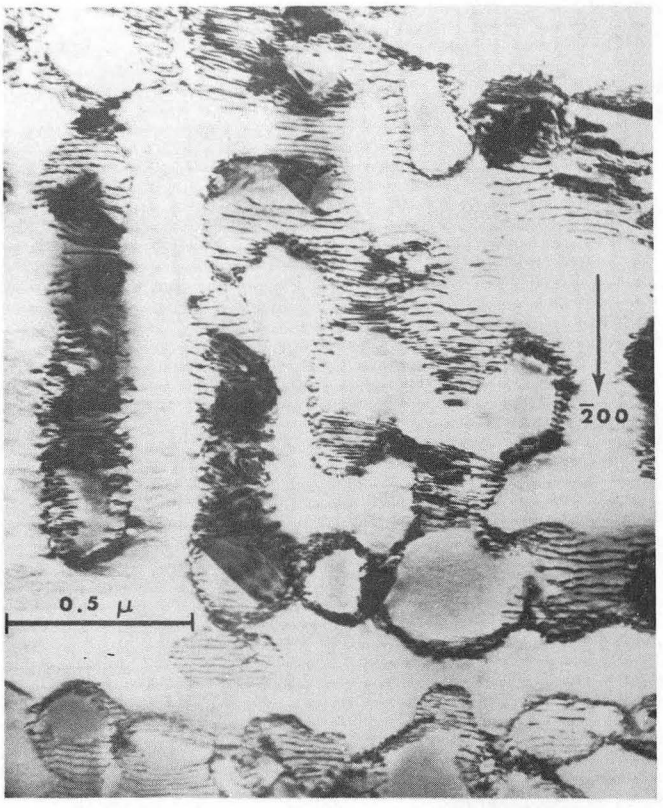

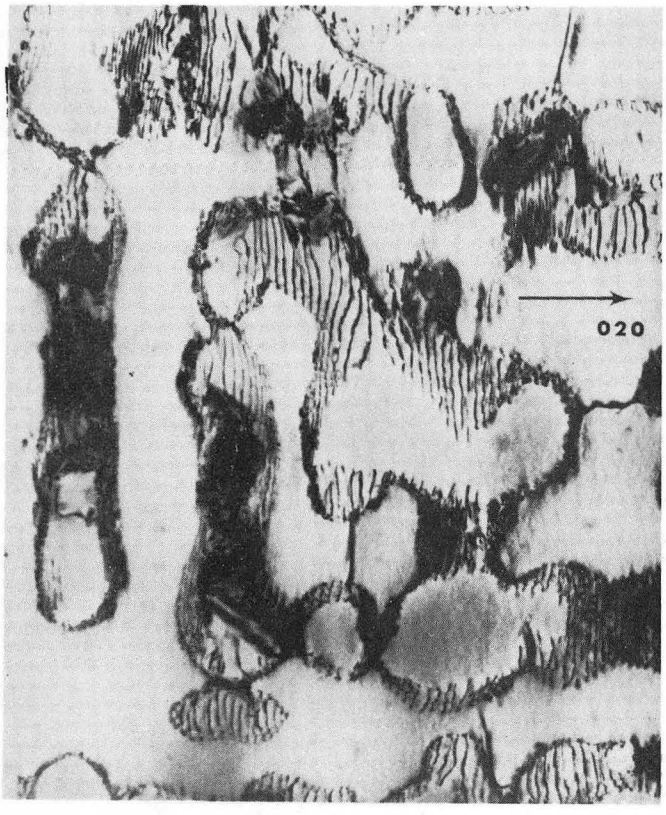

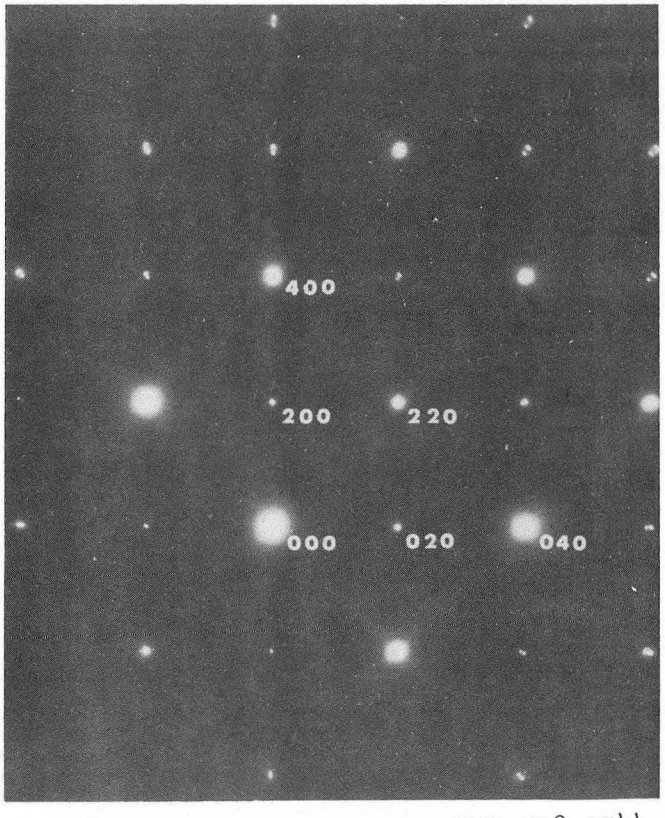

XBB 718-3544

Fig. 9

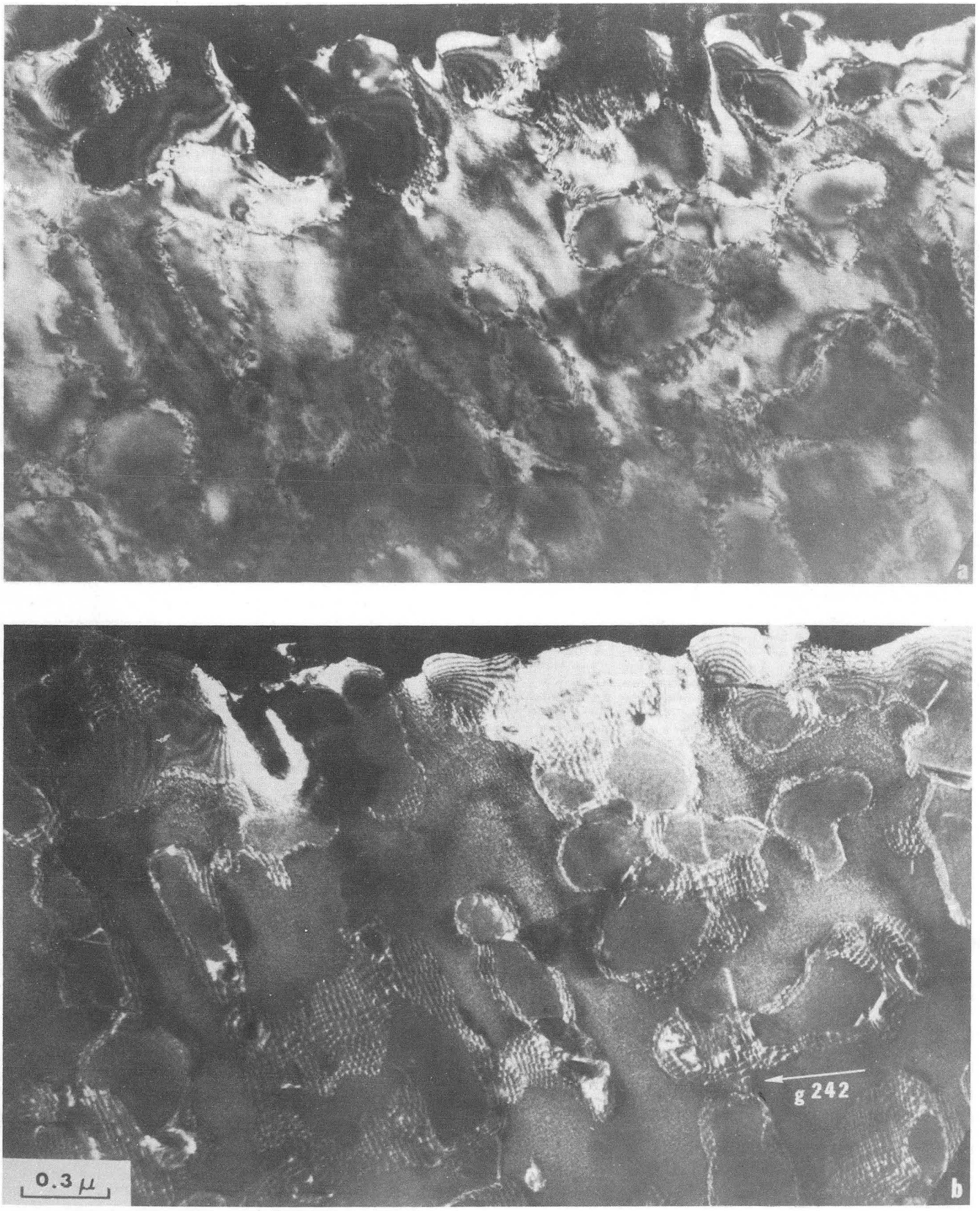

XBB 718-3724

Fig. 10

TECHNICAL INFORMATION DIVISION
LAWRENCE BERKELEY LABORATORY
UNIVERSITY OF CALIFORNIA
BERKELEY, CALIFORNIA 94720